MOLECULAR AND CELLULAR BIOLOGY, July 2000, p. 5248–5255 Vol. 20, No. 14
0270-7306/00/$04.00+0
Copyright © 2000, American Society for Microbiology. All Rights Reserved.

Delayed Wound Healing in Keratin 6a Knockout Mice

SONJA M. WOJCIK,[1] DONNIE S. BUNDMAN,[1] AND DENNIS R. ROOP[1,2]*

Department of Molecular and Cellular Biology[1] and Department of Dermatology,[2] Baylor College of Medicine, Houston, Texas 77030

Received 7 February 2000/Returned for modification 6 April 2000/Accepted 13 April 2000

Keratin 6 (K6) expression in the epidermis has two components: constitutive expression in the innermost layer of the outer root sheath (ORS) of hair follicles and inducible expression in the interfollicular epidermis in response to stressful stimuli such as wounding. Mice express two K6 isoforms, MK6a and MK6b. To gain insight into the functional significance of these isoforms, we generated MK6a-deficient mice through mouse embryonic stem cell technology. Upon wounding, MK6a was induced in the outer ORS and the interfollicular epidermis including the basal cell layer of MK6a$^{+/+}$ mice, whereas MK6b induction in MK6a$^{-/-}$ mice was restricted to the suprabasal layers of the epidermis. After superficial wounding of the epidermis by tape stripping, MK6a$^{-/-}$ mice showed a delay in reepithelialization from the hair follicle. However, the healing of full-thickness skin wounds was not impaired in MK6a$^{-/-}$ animals. Migration and proliferation of MK6a$^{-/-}$ keratinocytes were not impaired in vitro. Furthermore, the migrating and the proliferating keratinocytes of full-thickness wounds in MK6a$^{-/-}$ animals expressed neither MK6a nor MK6b. These data indicate that MK6a does not play a major role in keratinocyte proliferation or migration but point to a role in the activation of follicular keratinocytes after wounding. This study represents the first report of a keratin null mutation that results in a wound healing defect.

The ability of the epidermis to perform its function as a protective barrier is dependent to a significant degree on the presence and integrity of its keratin network. Keratin proteins form the intermediate filament cytoskeleton of epithelial cells (1, 12, 41). Keratins are subdivided into the slightly smaller acidic type I keratins and the larger more basic type II keratins (26). Type I and type II keratins are expressed in pairs, forming obligate heterodimers, which make up the basic building block from which the keratin filaments assemble (11, 40). Keratinocytes express different keratin pairs according to their state of differentiation. Cells in the basal compartment, which contains cells with proliferative capacity such as stem cells and transit-amplifying cells, express keratin 5 (K5) and K14. Postmitotic spinous keratinocytes are characterized by the expression of K1 and K10. A strict balance of proliferation, differentiation, and desquamation is normally maintained in the epidermis, but in case of an injury keratinocytes have the plasticity to exit this differentiation pathway and respond with migration and enhanced proliferation, forming a new epithelium to cover the wound. Under these circumstances a new set of keratins, K6, K16, and K17, is induced (30). A remarkable feature of K6 is that there have been descriptions of multiple functional K6 genes in several mammals; humans may have seven active K6 genes (43, 46), bovines may have up to three (5, 27), and mice have at least two (38, 44). In contrast to this, the assumed type I partners of K6, K16 and K17, appear to have only one functional gene and several pseudogenes (39, 45). While K6, K16, and K17 share the characteristic inducible expression in response to perturbations of epidermal homeostasis, their constitutive expression patterns are not identical. In hirsute skin, K6 and K16 are expressed constitutively in the innermost layer of the outer root sheaths (ORS) of hair follicles (38, 44, 46). This single-cell layer, also known as the companion cell layer, consists of highly differentiated flattened cells, which lie directly adjacent to Henle's layer of the inner root sheath (14, 15, 29). K17, on the other hand, is expressed early during embryonic development prior to formation of the hair follicle placodes in the single-layer ectoderm and is later present in the entire ORS of mature hair follicles as well as in sweat and sebaceous glands (24, 31). In addition to this, some body sites devoid of hair express K6 and K16 and K17 to various degrees, such as palms, soles, and the nail bed, as do several mucous epithelia such as the oral cavity, esophagus, trachea, and the vaginal, and anal epithelia (26). Both murine K6 isoforms, MK6a and MK6b (designated MK6α and MK6β, respectively, by Takahashi and colleagues (44)), are expressed in the footpad and oral epithelia, and both are induced after wounding or treatment with phorbol esters (38, 44). However, inducible expression of MK6b in the epidermis has been reported to be more suprabasal than that of MK6a, and MK6a but not MK6b has been shown to be expressed in the companion cell layer of the hair follicle (38, 44).

The integral role that keratin filaments play in the maintenance of the structural integrity of the epidermis has now been well established, with a large number of reports which document keratin mutations, including mutations affecting K6, K16, and K17, as the cause of several inherited genodermatoses (for a recent review see reference 7). Apart from its role in human disease, K6, because of its unique expression characteristics, is a fascinating subject for the experimental study of keratin function. Elucidation of the significance of K6 expression in wound healing or its function in the epithelia with constitutive expression would not only further our understanding of K6 but also potentially provide insight into the biological necessity of having different sets of keratins for different cell types. We have shown that expression of dominant-negative mutants of K6 in the companion cell layer leads to the destruction of these cells (47), and Takahashi and colleagues reported on inducible skin blistering after induction of a dominant-negative K6 transgene in the epidermis (42). However, the functional significance of a protein is sometimes better evaluated by analyzing the consequences of its absence. To date, several keratin

* Corresponding author. Mailing address: Department of Molecular and Cellular Biology, Baylor College of Medicine, One Baylor Plaza, Houston, TX 77030. Phone: (713) 798-4966. Fax: (713) 798-3800. E-mail: roopd@bcm.tmc.edu.

knockout models have been generated, and the resulting phenotypes mostly underscore the role keratins play in providing mechanical support to epithelial cells. Mice lacking a functional MK10 gene (33) and MK14-deficient mice (21) exhibit epidermal lesions. MK4-deficient mice suffer from fragility in internal epithelia (28), and MK12 knockouts display corneal defects (17). Targeting of the embryonic keratins MK8 and MK18 provided results less clear-cut with respect to keratin function. Deletion of MK8 led to midgestational lethality (3) or colorectal hyperplasia (2), depending on the genetic background. Targeting of the type I partner of MK8, MK18, resulted in liver pathology apparent only in older mice (22).

We have targeted the MK6a gene, deleting the entire coding region through homologous recombination in embryonic stem (ES) cells. MK6a-deficient mice have no apparent structural defects in hair follicles, footpads, oral epithelia, or the periderm. They do however exhibit a delay in reepithelialization from the hair follicle after superficial wounding but not in the healing of full-thickness wounds. The lack of MK6a affects both proliferation and migration of the follicular keratinocytes in vivo, but not proliferation or migration of MK6a$^{-/-}$ keratinocytes in vitro. These data indicate that MK6a$^{-/-}$ keratinocytes may not be impaired in proliferation or migration as such but rather in the activation of one or both. This is the first report of a keratin null mutation where the phenotypic consequences do not appear related to the structural deterioration or hyperplastic response of the affected cells.

MATERIALS AND METHODS

Targeting-vector construction. PCR primers 5′-CTGCTATTGCTGATGCTG AG-3′ and 5′-GTCCAACACCTTCACCATTC-3′ were used to identify P1 clones from the Genome Systems 129/SvJ library that contained both the MK6a and the MK6b genes. The MK6a gene was subcloned and confirmed by restriction mapping and spot sequencing. To generate the 5′ arm of the targeting vector, a 5-kb *Sal*I-*Xba*I fragment directly 5′ to the MK6a coding sequence was ligated to the hprtΔ3′-neo cassette (35), which contains the 5′ half of a hypoxanthine phosphoribosyltransferase minigene and a neomycin cassette. For the 3′ arm, a 3.2-kb *Ava*I-*Bam*HI fragment directly downstream of the MK6a stop codon was subcloned to pick up a *Not*I restriction site. The MK6a targeting vector was constructed by the simultaneous ligation of the following four fragments: a 9.7-kb *Sal*I-*Not*I fragment containing the previously ligated 5-kb 5′ arm and the hprtΔ3′-neo cassette, a 3.2-kb *Not*I-*Bam*HI fragment that constitutes the 3′ arm, a 2.1-kb *Bam*HI-*Hin*dIII fragment containing a thymidine kinase cassette (provided by John Lydon, Baylor College of Medicine), and the 3-kb pSK(−) backbone cut with *Hin*dIII and *Not*I. The resulting 18-kb targeting vector was transformed into SureTM cells (Stratagene) and prepared by CsCl centrifugation. Prior to electroporation, the targeting vector was linearized with *Sal*I.

Generation of MK6a knockout mice. Mouse ES cells (129/SvEv AB2.2) and the feeder cell line SNL76/7 (25) were kindly provided by Allan Bradley, Baylor College of Medicine. Electroporation, cell culture, drug selection, expansion of clones in 96-well plates, and Southern screening of ES cell DNA were performed according to published protocols (34, 36). DNA for Southern analysis was digested with *Eco*RV and probed with a 0.9-kb *Bgl*II-*Sal*I fragment that lies just outside the 5′ arm of the targeting vector (see Fig. 1a). The 3′ end of the targeted locus was confirmed by PCR analysis using primers 5′-GGTGGCCTCAGCTC TTCTAC-3′, 5′-AGATCCACTAGTTCTAGCCTCG-3′, and 5′-ACAGGCAG CCTCAGAGACAG-3′ (Fig. 1a and c). Chimeras were generated by injection of targeted ES cells into C57BL/6N blastocysts.

Animal protocols. Mice were kept under standard housing conditions at the animal facility at Baylor College of Medicine. Wound-healing protocols were approved by the Center for Comparative Medicine. Mice were anesthetized using 0.0175 ml of 2.5% Avertin per g of mouse. For the duration of each wound-healing experiment acetaminophen (Children's Tylenol) was added to the drinking water at 1 mg/ml and sulfamethoxazole/trimethoprim oral suspension (Apothecon) was added at 1 ml/150 ml. For tape-stripping wounds, mice were shaved and two 1- to 1.5-cm^2 areas to the left and right of the spine were depilated with Nair (Carter-Wallace). The depilated areas were tape stripped eight times with Tesa tape (Bron Tape) and immediately wiped with Betadine solution. Full-thickness wounds were generated in the center of the lower back after shaving and wiping with Betadine solution. A circle 5 mm in diameter was marked on the skin using a biopsy punch dipped in methylene blue solution and subsequently excised using curved scissors. Wound-healing samples were analyzed histologically from five +/+ and five −/− animals per time point for both tape-stripping and full-thickness wounds. Tape stripping was considered successful if a crust had formed on top of the dermis without any inflammatory infiltrate within the dermis. Samples that did not have an intact, superficial crust were excluded from the analysis. Reepithelialization of tape-stripping wounds was scored visually according to the continuity and thickness of the epithelium growing under the crust. Full-thickness wounds were assessed according to the lengths of the epithelial tongues migrating from both edges of the wound.

BrdU labeling. In vivo bromodeoxyuridine (BrdU) labeling of wounded mice was carried out by intraperitoneal injection of 0.01 ml of a 10-mg/ml solution of BrdU triphosphate (Sigma) per gram of mouse. Mice were sacrificed 2 h after the BrdU injection. Samples were prepared as described below. For tape-stripping wounds BrdU-positive cells in the follicles of a series of tissue sections were counted. A minimum of 300 follicles (sections) were counted for each data point presented in Table 1, and the standard deviations (SD) were calculated.

RNase protection analysis. Total RNA was isolated from ear skin with RNAzol B (Tel-Test) 48 h after a single application of 50 μl of 0.1-mg/ml 12-*O*-tetradecanoyl-phorbol-13-acetate in acetone. The RNA probe for MK6 detects both MK6a and MK6b and has been described previously (38). RNA probes for MK6 and cyclophilin (Ambion) were generated using the Riboprobe Gemini II kit (Promega). The RNase protection assay was performed with the RPA II kit (Ambion), with overnight hybridization at 42°C.

Western blot analysis. Tissue samples were ground in liquid N_2 and then solubilized, electrophoresed, and blotted onto nitrocellulose as previously described (4). Blots were blocked with 5% nonfat milk–Tris-buffered saline and then probed with rabbit anti-K6, sheep anti-K14 (37), and guinea pig anti-K6 (38), followed by alkaline phosphatase-conjugated anti-rabbit immunoglobulin G (IgG) (Boehringer Mannheim), anti-sheep IgG (Zymed), and anti-guinea pig IgG (Zymed), respectively. Bands were visualized using nitroblue tetrazolium-BCIP (5-bromo-4-chloro-3-indolylphosphate) solution (Boehringer Mannheim) according to the manufacturer's instructions.

Histology. Pieces of tissue were flattened onto filter paper and fixed overnight in Carnoys' solution (ethanol-chloroform-glacial acetic acid; 6:3:1). Samples were then washed in 100% ethanol and processed for paraffin embedding, and the blocks were sectioned at 5 to 6 μm in thickness. Sections were deparaffinized through a graded series of xylenes and ethanol and either stained with hematoxylin and eosin or rinsed twice for 10 min in phosphate-buffered saline (PBS) and incubated with the appropriate antibodies. BrdU-labeled samples were incubated for 12.5 min in 25% HCl following deparaffinization and one 10-min incubation in PBS and then rinsed three times for 10 min in PBS prior to incubation with the antibodies. Samples for frozen sections were prepared as previously described (4).

Primary keratinocyte culture. Primary keratinocytes were isolated and cultured as previously described (4). Keratinocytes of 1- to 3-day-old MK6a$^{-/-}$ and MK6a$^{+/+}$ littermates were plated at 10^5 cells per cm^2 in low-Ca^{2+} medium (50% Eagle minimal essential medium without Ca^{2+} (Gibco BRL) and 50% fibroblast-conditioned medium (10) with final concentrations of 0.05 mM Ca^{2+}, 8% fetal bovine serum, and 4 ng of epidermal growth factor/ml).

[^{3}H]thymidine incorporation. Keratinocyte cultures were plated in triplicate, refed at 24 h, and allowed to grow in low-Ca^{2+} medium for a total of 46 h. [^{3}H]thymidine was diluted into the medium to a final concentration of 1 μCi/ml, and the cells were grown in its presence for 2 h. The cultures were then washed three times with PBS and incubated with 8% trichloroacetic acid for 5 min, followed by two brief washes with 8% trichloroacetic acid. The cells were then solubilized in 1 N NaOH for 30 min, and the solution was neutralized by adding 1 N HCl. The samples were counted in a scintillation counter. The cell number 24 h after plating was assessed for each batch of cells in triplicate with a modified crystal violet staining procedure (9). The scintillation counts were then adjusted for the cell number.

Double-label immunofluorescence. All sections were blocked with 1% bovine serum albumin in PBS for 30 min. Two-color immunofluorescence was performed by sequential incubation with primary antibodies and fluorescein isothiocyanate (FITC)- or Texas red (TxRed)-conjugated secondary antibodies. Primary antibodies used were rabbit anti-K6, rabbit anti-K14, guinea pig anti-K14 (37), and rabbit anti-MK16 (32). Furthermore, a guinea pig anti-K6 antibody (38), which in mice is specific for MK6b, and guinea pig anti-K6 generated to the synthetic peptide CGSKKSYRQ (corresponding to a CG linker peptide and the last seven amino acids of MK6a) were used. Secondary-antibody conjugates used were anti-rabbit FITC (Dako) and anti-guinea pig TxRed (Vector). For BrdU-labeled samples the primary keratin antibody was diluted into the FITC-conjugated anti-BrdU (Becton Dickinson) followed by a second incubation with anti-guinea pig TxRed (Vector).

RESULTS

Deletion of the entire MK6a coding region from the genome. Initial Southern analysis of two overlapping P1 clones containing the MK6 locus indicated that there might be as many as five MK6 genes, the MK6a and MK6b genes and three additional genes similar to K6 which lie downstream of the MK6b gene (data not shown). We decided to target the MK6a gene, since previous analysis of MK6a and MK6b transgene expression

had indicated that MK6a was the most widely expressed isoform (38). The targeting vector was designed to replace the entire MK6a coding sequence with a neomycin resistance selection cassette as well the 5′ half of an hprt minigene and a *lox*P site; the complete cassette is designated hprtΔ3′-neo (Fig. 1a). This cassette was used because it would allow us to delete the entire MK6 locus with a second targeting event followed by transfection with a cre recombinase expression vector, should the MK6 genes downstream of MK6b prove to be active (for a more detailed explanation of this targeting strategy see reference 35). The MK6a replacement vector was introduced into 129/SvEv AB2.2 ES cells. Successful gene targeting was confirmed by Southern blotting, using a 5′ external probe (Fig. 1b) as well as an internal probe to the neomycin cassette (data not shown). Germ line transmission was obtained from chimeras of two independent clones, and one clone was selected for subsequent analyses. Matings of MK6a$^{+/-}$ animals produced all genotypes, +/−, +/+, and −/−, at the expected Mendelian ratio. Offspring from heterozygous crosses were screened using a set of three primers to the 3′ end of the targeted locus (Fig. 1a and c). MK6a-deficient mice were indistinguishable from their wild-type and heterozygous littermates at birth and grew hair synchronously with their littermates. Subsequent hair cycles also showed no abnormalities in onset or duration. Older MK6a$^{-/-}$ mice (1.5 years) showed no abnormal deterioration of coat, mucous epithelia, or footpad compared to wild-type animals of the same age and genetic background. The absence of the MK6a transcript in MK6a$^{-/-}$ mice was confirmed by RNase protection analysis (Fig. 1d). Western blot analysis of whole-skin samples taken on postnatal day 16, when the hair follicles were in anagen, showed that MK6a was absent in MK6a$^{-/-}$ samples (Fig. 1e, left). The MK6 antibody used for the left panel was raised to the C terminus of MK6a and did not recognize MK6b after denaturation but did detect MK6b on unfixed frozen sections of MK6a$^{-/-}$ samples. Use of another K6 antibody, which in mice reacts only with MK6b (anti-MK6b) (38) (Fig. 1e, middle) revealed that MK6b was expressed at considerably lower levels than MK6a in both the MK6a$^{+/+}$ and MK6a$^{-/-}$ mice. MK6b was also expressed at significantly lower levels than MK6a in the periderm and telogen hair follicles (data not shown). There were no differences in the protein levels of MK6b between MK6a$^{+/+}$ and MK6a$^{-/-}$ mice in any of the samples tested.

MK6a and MK6b are expressed in the companion cell layer and the periderm. To confirm that MK6b expression detected in whole skin by Western blot analysis was due to expression in the companion cell layer, we performed immunofluorescence analysis utilizing the anti-MK6b antibody. MK6b was expressed in the companion cell layer of telogen hair follicles of both MK6a$^{-/-}$ (Fig. 2a) and MK6a$^{+/+}$ (Fig. 2a, inset) animals, as well as in the companion cell layers of anagen hair follicles of both genotypes (Fig. 2b). The same MK6b-specific antibody used on embryonic-day-16.5 skin showed that MK6b was also expressed in the periderms of both MK6a$^{+/+}$ (Fig. 2c) and MK6a$^{-/-}$ (Fig. 2d) mice. The constitutive expression pattern observed for MK6b in the hair follicle and periderm is identical to the expression pattern of MK6a in these compartments (38).

MK6a but not MK6b is inducible in the basal compartment of the epidermis and the outer ORS of the hair follicles. Our previous analysis of expression of MK6b constructs in transgenic animals (38), as well as in situ hybridization reported by Takahashi and colleagues (44), had already indicated that MK6b induction in the epidermis is suprabasal. Immunofluorescence analysis of inducible MK6 expression at the edge of a wound in MK6a$^{+/+}$ animals showed MK6 induction throughout the entire epidermis and ORS (Fig. 2e). In contrast to this,

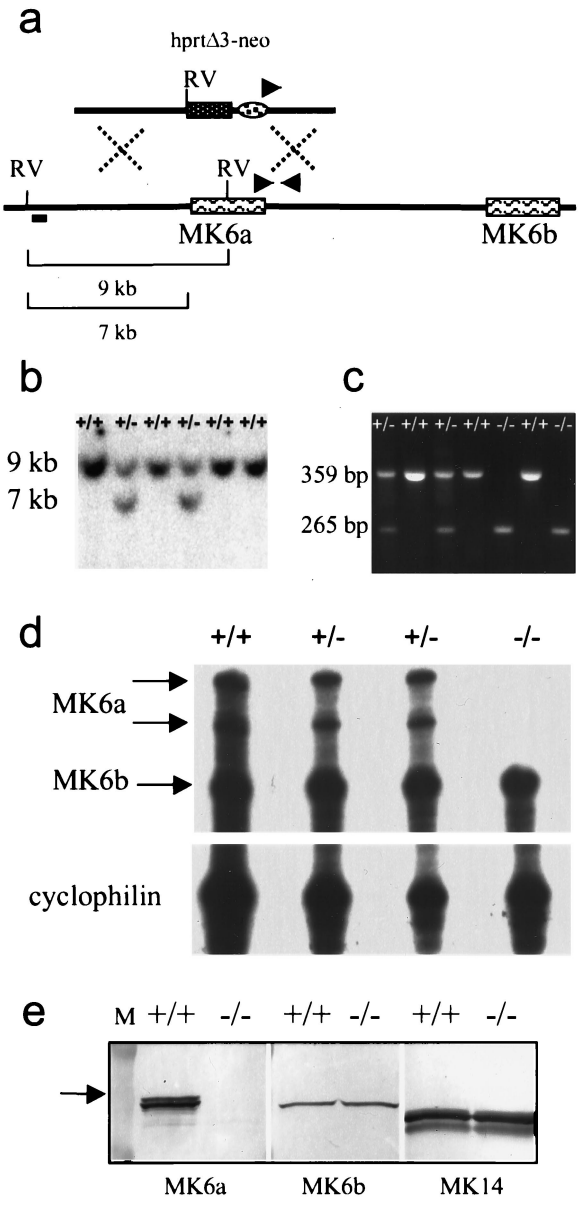

FIG. 1. Targeting of MK6a. (a) A replacement vector containing the hprtΔ3′-neo cassette was used to delete the MK6a coding region through homologous recombination. RV, *Eco*RV restriction sites, digestion of which generates a 9-kb fragment for the wild-type locus and a 7-kb fragment for the targeted allele; short bar, position of the 5′ external probe; triangles, positions of the PCR primers used in the 3′ screen. (b) Genomic Southern blot showing the wild-type 9-kb and the targeted 7-kb fragments detected with the 5′ external probe. (c) Genomic PCR of the 3′ end of the targeted locus showing a 359-bp product for the MK6a$^{+/+}$ genotype, a 265-bp product for MK6a$^{-/-}$, and both fragments for MK6a$^{+/-}$. (d) RNase protection assay showing absence of the MK6a transcript in MK6a$^{-/-}$ animals. The RNA was isolated from the 12-*O*-tetradecanoyl-phorbol-13-acetate-treated ears of littermates. The probe was designed to protect 268 bases in MK6b and 382 bases in MK6a. Note that two bands are generated for the MK6a transcript, most likely due to a polymorphism present in the C57BL/6N strain, resulting in partial degradation of the 382-bp fragment. The probe spans exons three to six, and a single MK6a band was observed in BALB/c mice, the strain from which the cDNA was isolated. A cyclophilin probe was used as a loading control. (e) Western blot analysis of whole skin during anagen showing that MK6a is absent in MK6a$^{-/-}$ mice (left). Note that MK6b is present at lower levels than MK6a and is not upregulated in MK6a$^{-/-}$ mice (middle). MK14 was used as a loading control (right). Note that the doublet bands for MK6a and MK14 most likely are due to differential phosphorylation. Lane M, 84- and 51-kDa size marker bands; arrow, position of the 62.5-kDa band.

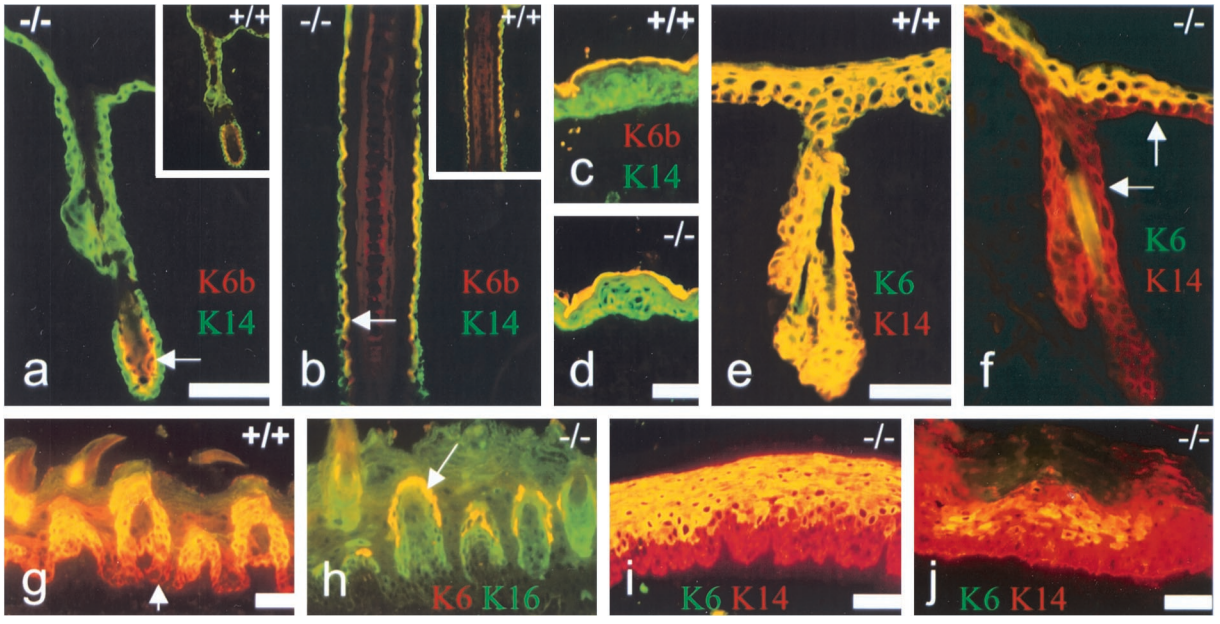

FIG. 2. Immunofluorescence analysis showing MK6a and MK6b expression patterns. (a through d) MK14 staining in green (FITC) and the overlapping MK6b staining in yellow (TxRed). (a) MK6b (yellow) is present in the companion cell layer (arrow) of telogen hair follicles in MK6a$^{-/-}$ animals and MK6a$^{+/+}$ animals (inset). (b) MK6b (yellow) expression in the companion cell layer (arrow) of anagen hair follicles in MK6a$^{-/-}$ and MK6a$^{+/+}$ mice (inset). Note that the outer ORS is only one cell layer thick in this section and only positive for MK14 (green); the outer ORS and the MK6b-positive companion cell layer are most readily distinguished in the lower part of the section (arrow). (c and d) MK6b is expressed in the periderm (yellow) of embryonic day 16.5 skin of MK6a$^{+/+}$ and MK6a$^{-/-}$ animals. Note that the periderm is a single-cell layer covering the developing epidermis, which is highlighted by the MK14 antibody in green. (e and f) Samples taken from the edge of 34-h-old tape-stripping wounds. MK14 staining (TxRed) highlights the epidermis and the ORS of the hair follicles. (e) MK6 induction (yellow) in MK6a$^{+/+}$ animals is apparent in the entire epidermis and the ORS of the hair follicle. (f) MK6b in MK6a$^{-/-}$ animals is induced in the suprabasal layers of the epidermis but not in the basal layer of the epidermis or the ORS (arrows). Note that MK6b staining is not seen in the companion cell layer of the follicle because the antibody used here for comparison with the MK6a$^{+/+}$ sample does not recognize MK6b in the companion cells of fixed tissue but recognizes it on unfixed frozen sections (not shown). (g) MK6a is expressed throughout the dorsal tongue epithelium in MK6a$^{+/+}$ animals (TxRed). The antibody recognizes both MK6a and MK6b. The overlapping yellow staining shows the suprabasal expression of MK16 in the papillae. Note that in the basal layers (arrow) MK6a (red) is expressed but not MK16. (h) MK6b (yellow) is restricted to the uppermost cells of the papillae in MK6a$^{-/-}$ animals. The MK16 staining (green) in the MK6a$^{-/-}$ tongue epithelium is identical to the MK16 staining seen in the MK6a$^{+/+}$ sample. (i) MK6b (yellow) is expressed suprabasally in the hard palate (counterstained with MK14; TxRed) in MK6a$^{-/-}$ mice. (j) Suprabasal MK6b expression in MK6a$^{-/-}$ footpad, which was counterstained with MK14 (TxRed). Note that MK6 expression in the footpad is patchy. (a, b, e, and f) Carnoys fixed samples; (c, d, and g to j) unfixed frozen sections. Scale bars, 50 μm.

in MK6a$^{-/-}$ mice no inducible MK6 expression in either the basal layer of the epidermis or the outer layers of the ORS of the hair follicles was observed (Fig. 2f). This confirmed unequivocally that in mice the MK6a isoform alone is responsible for inducible MK6 expression in the basal layer of the epidermis as well as the outer ORS, while MK6b can only be induced in the suprabasal layers of the epidermis. Constitutive expression of MK6b in tongues (Fig. 2h), palates (Fig. 2i), and footpads (Fig. 2j) of MK6a$^{-/-}$ mice was also suprabasal, whereas wild-type mice showed MK6 expression in all layers of these epithelia (data for MK6a$^{+/+}$ palates and footpads are not shown). Interestingly, the expression of MK6a in wild-type mice was observed throughout the entire dorsal epithelium of the tongue, whereas MK16 expression was more suprabasal and restricted to the papillae (Fig. 2g). MK6b expression in the tongues of MK6a$^{-/-}$ mice was also restricted to the papillae, but, unlike MK16, MK6b was only present in the cells at the very upper edge of these structures (Fig. 2h).

MK6a$^{-/-}$ mice show a delay in reepithelialization from the hair follicle. If the epidermis of adult mice is destroyed by abrasion, reepithelialization occurs from the hair follicle epithelium. Because MK6a$^{-/-}$ mice lack inducible MK6 expression in the outer ORS, we analyzed the kinetics of reepithelialization in MK6a$^{+/+}$ and MK6a$^{-/-}$ mice in an abrasion wound model. The epidermis was destroyed by tape stripping (eight times with Tesa tape) of shaved, depilated back skin. This procedure removes the suprabasal cell layers and leaves behind but kills the basal layer. A crust then forms under the dead basal layer, and reepithelialization occurs from the hair follicles, with the new epidermis forming under the crust. Tape stripping during telogen, when the hair follicles are not deeply anchored in the dermis, proved to be problematic. Although some samples showed less reepithelialization in MK6a$^{-/-}$ than in MK6a$^{+/+}$ mice, the majority of samples in these experiments had to be discarded because tape stripping during telogen often damaged the underlying connective tissue so severely that reepithelialization occurred from the edge of the wound rather that from the hair follicles (data not shown). During anagen, the active growth phase, the hair follicles reach down deep into the hypodermis, stabilizing the skin during tape stripping. In anagen, keratinocytes in the ORS are actively dividing. Tape stripping during anagen revealed no obvious differences between MK6a$^{+/+}$ and MK6a$^{-/-}$ mice at 23 h after wounding (data not shown).

To avoid the skin fragility problems of telogen and the activated ORS keratinocytes of anagen hair follicles, mice were tape stripped in late catagen, when the hair follicles have almost completely regressed but are still deep enough to stabilize the dermis. C57BL/6N (F4) mice were tape stripped during their second catagen, at the age of 39 to 45 days. Since the second hair cycle is not as perfectly synchronized as the first one is, each mouse was checked for the progression of the second anagen over the back, as judged by the disappearance of pigmentation from the back skin. Tape stripping of the

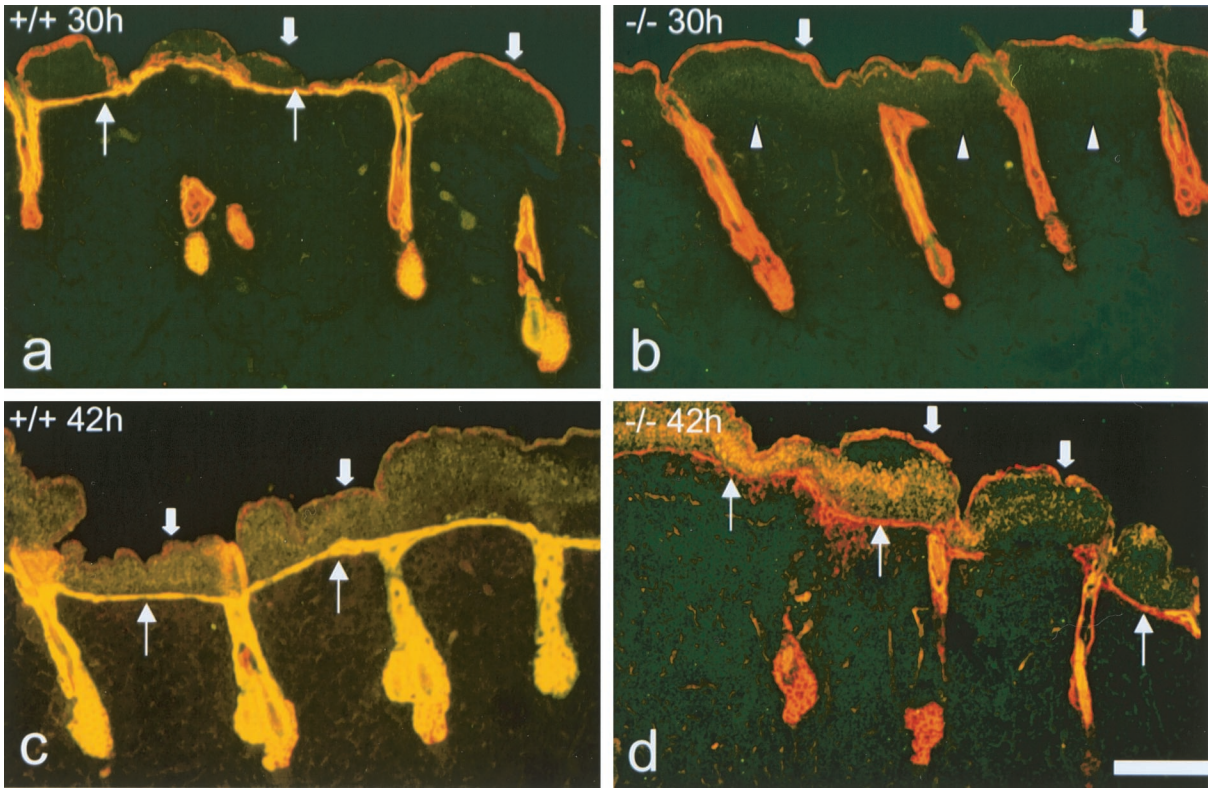

FIG. 3. Immunofluorescence analysis of reepithelialization after tape stripping. All samples were stained with antibodies to MK14 (red) and MK6 (yellow). The dead old basal layer is still present on top of the crust (thick arrows) and is positive for MK14 but negative for MK6. (a) MK6a$^{+/+}$ animals show some areas of reepithelialization 30 h after tape stripping. A single-cell layer, positive for MK6, is apparent under the crust (thin arrows). Note the induction of MK6a in the ORS of the hair follicles. (b) MK6a$^{-/-}$ mice show no reepithelialization from the hair follicles 30 h after tape stripping. Arrowheads, boundary of crust and dermis; thick arrows, old basal layer on top of the crust. (c) MK6a$^{+/+}$ samples taken 42 h after tape stripping show a continuous epithelium of two to four cell layers under the crust (thin arrows). (d) MK6a$^{-/-}$ samples taken 42 h after tape stripping show a discontinuous mostly single-cell layer epithelium under the crust (thin arrows). Note that the follicular cells that reach the dermal surface do not induce MK6b until a suprabasal layer is present. Scale bar, 100 μm.

epidermis at this stage was successful, and MK6a$^{-/-}$ mice showed a clear delay in reepithelialization from the hair follicles compared to MK6a$^{+/+}$ mice (Fig. 3 and 4). In MK6a$^{+/+}$ mice, at 30 h after tape stripping a single layer of new epithelium could be observed in some areas under the crust (Fig. 3a and 4a). By 34 h, the cell layer became continuous and one to three cells thick (not shown), and by 42 h the new epithelium had thickened to two to four cell layers (Fig. 3c and 4c). In MK6a$^{-/-}$ mice no reepithelialization was observed at 30 h (Fig. 3b and 4b), but by 34 h the first follicular keratinocytes had reached the dermal surface (not shown). By 42 h MK6a$^{-/-}$ mice showed a discontinuous new epithelium one or two cell layers thick (Fig. 3d and 4d), which was easily distinguishable from the thicker epithelium present at this time point in wild-type mice (Fig. 3c and 4c). Two days after wounding, MK6a$^{-/-}$ mice had also formed a continuous multilayered epithelium and the MK6a$^{-/-}$ samples became harder to distinguish from the MK6a$^{+/+}$ samples (data not shown).

Both migration and proliferation of MK6a$^{-/-}$ follicular keratinocytes are delayed in vivo. In an attempt to define whether the delay in reepithelialization from the hair follicle in MK6a$^{-/-}$ mice was due to a defect in migration or proliferation of MK6a-deficient follicular keratinocytes, mice were injected intraperitoneally with BrdU triphosphate 2 h prior to being sacrificed. If the delay were solely due to an impairment of migration, one might have predicted a buildup of labeled follicular keratinocytes in MK6a$^{-/-}$ mice. In both MK6a$^{+/+}$ and MK6a$^{-/-}$ mice proliferation of follicular keratinocytes and their migration out of the follicle appeared to be closely linked. At the 34-h time point, when MK6a$^{+/+}$ mice showed a continuous one- to three-cell layer epithelium and reepithelialization was just beginning in MK6a$^{-/-}$ animals, we counted fewer BrdU-labeled cells per follicle in MK6a$^{-/-}$ mice than in MK6a$^{+/+}$ mice (Table 1). At 42 h, when the MK6a$^{+/+}$ mice had formed a continuous two- to four-cell layer epithelium and MK6a$^{-/-}$ animals had formed a discontinuous single-layer epithelium, the number of labeled follicular keratinocytes had increased for both genotypes but the labeling index for MK6a$^{-/-}$ follicles was still lower (Table 1).

Full-thickness wounds in MK6a$^{-/-}$ mice heal without delay. Since the lack of MK6a in the follicular keratinocytes in MK6a$^{-/-}$ mice seemingly caused a delay in the migration of those cells out of the follicle, we next tried to determine whether the absence of MK6a in basal epidermal keratinocytes would impair the migration of the epithelial tongue into a full-thickness wound bed. Full-thickness wounds were created on the lower backs of C57BL/6N (F4) mice during telogen. Mice were sacrificed, and the wounds were excised on days 1 to 3, 5, and 7 after wounding. Histological analysis revealed no differences in the progress of the epithelial tongue from the edge of the wound between MK6a$^{+/+}$ and MK6a$^{-/-}$ animals (data not shown). Immunofluorescence analysis of day 5 wounds showed MK6 staining throughout the newly forming epithelium in wild-type mice (Fig. 5a), whereas MK6b was not present in the basal three or four layers in MK6a$^{-/-}$ animals (Fig. 5b). MK16 was expressed suprabasally in the migrating

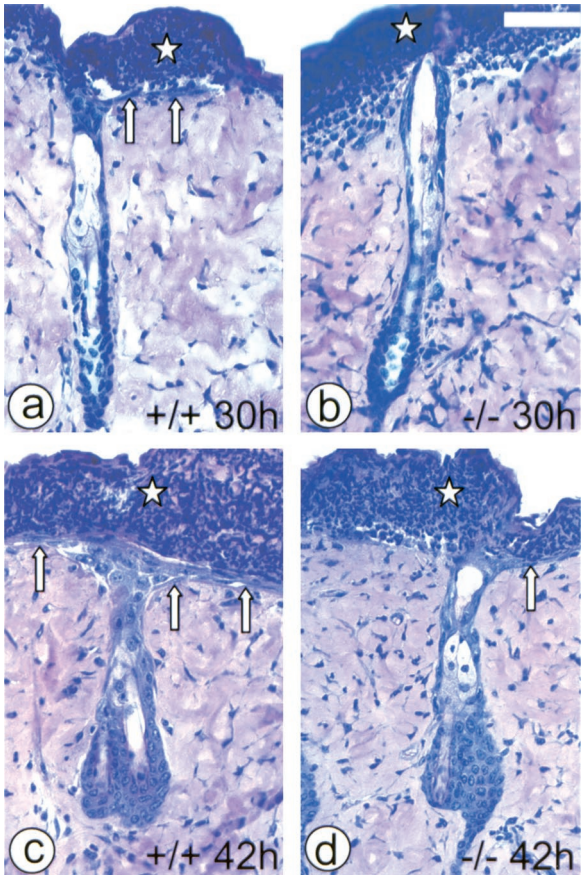

FIG. 4. Histological analysis of reepithelialization after tape stripping. Star, crust covering the denuded dermis; arrows, new epithelium regrowing from the hair follicles. (a) MK6a$^{+/+}$ follicle 30 h after tape stripping with a single-cell layer of new epithelium (arrows) beginning to grow out from the follicle. (b) MK6a$^{-/-}$ follicle 30 h after tape stripping without any sign of reepithelialization. (c) MK6a$^{+/+}$ follicle 42 h after wounding with a newly formed epithelium (arrows), which is two to four cell layers thick. Note that the thickest part of the epithelium can be found above the follicle. (d) MK6a$^{-/-}$ follicle 42 h after tape stripping with a single-cell layer of new epithelium (arrow) on one side of the follicle. Scale bar, 50 μm.

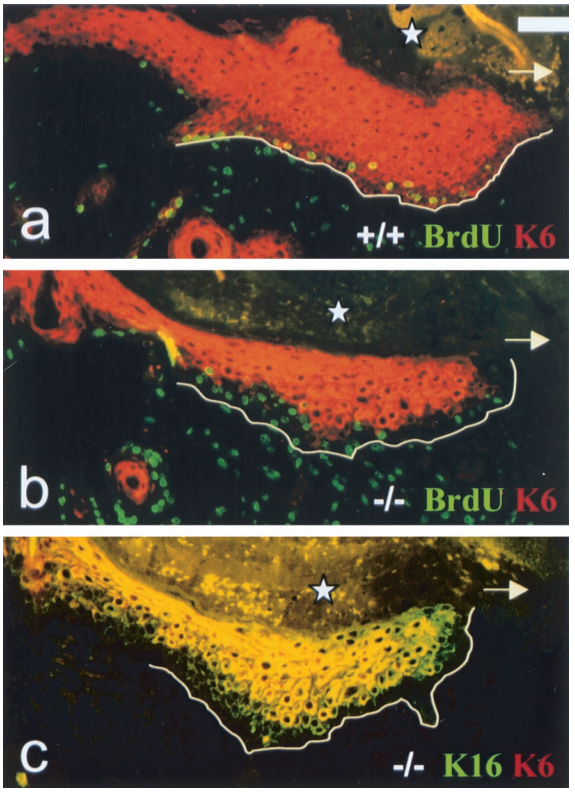

FIG. 5. Immunofluorescence analysis of full-thickness wounds. Arrow, direction of migration of the epithelial tongue; star, crust covering the wound; line, boundary of the migrating epithelial tongue and the granulation tissue. (a) MK6a$^{+/+}$ 5-day-old full-thickness wound. All layers of the migrating epithelial tongue are MK6 positive (red). Note that in order to show a well-preserved wound, fixed tissue, on which this MK6 antibody results in weaker staining of the basal layers, is shown; however, this is not the case on unfixed frozen sections (not shown). Proliferating keratinocytes in the bottom layers of the epithelial tongue are BrdU (FITC) and MK6a (TxRed) positive and therefore appear to have yellow nuclei. The proliferating cells in the granulation tissue are only BrdU positive, and the nuclei appear green. (b) MK6a$^{-/-}$ 5-day-old full-thickness wound. Note that the BrdU-positive, proliferating keratinocytes are negative for MK6b. (c) Double staining for MK16 (FITC) and MK6 (TxRed) in MK6a$^{-/-}$ animals reveals that MK16 is induced in cells below those expressing MK6b. Scale bar, 50 μm.

tongue and double staining for MK16 and MK6 in MK6a$^{-/-}$ animals revealed that MK16 induction occurs in cells below those expressing MK6b (Fig. 5c). The absence of MK6 in the bottom layers and the very tip of the epithelial tongue does not appear to impair the ability of the keratinocytes to migrate out into the wound bed. In vivo BrdU labeling of day-5 full-thickness wounds showed proliferating cells in the three or four basal cell layers (Fig. 5a and b). In MK6a$^{-/-}$ mice the BrdU-positive layers of the epithelial tongue did not express MK6b.

TABLE 1. Numbers of BrdU-positive cells in follicle sections[a]

Time (h)	Avg no. of BrdU-positive cells counted per follicle section ± SD for mice of genotype:	
	+/+	−/−
34	2.75 ± 0.14 2.66 ± 0.17	1.66 ± 0.11 2.16 ± 0.22
42	5.24 ± 0.35 5.56 ± 0.36	4.21 ± 0.14 4.66 ± 0.31

[a] Listed are the counts from two animals per time point and genotype.

The fact that BrdU staining and suprabasal MK6b staining in the MK6a$^{-/-}$ sample do not overlap (Fig. 5b) indicates that in vivo MK6b, unlike MK6a (Fig. 5a), is not expressed in the keratinocytes that proliferate after wounding.

Proliferation and migration of MK6a$^{-/-}$ keratinocytes are not affected in vitro. Since MK6a$^{-/-}$ follicles showed lower labeling indices, we compared the abilities of MK6a$^{+/+}$ and MK6a$^{-/-}$ keratinocytes to proliferate in vitro. Incorporation of [^{3}H]thymidine resulted in values of 2,661 cpm (standard deviation [SD], 163) for MK6a$^{+/+}$ cultures and 2,527 cpm (SD, 76) for MK6a$^{-/-}$ cultures, indicating that there was no significant difference in the proliferation rates in vitro. Migration of MK6a$^{+/+}$ and MK6a$^{-/-}$ keratinocytes in vitro was tested on collagen type I, collagen type IV, fibronectin, and laminin substrates by assessing gap closure rates of scrape wounds (data not shown). No differences in the migration rates of MK6a$^{+/+}$ and MK6a$^{-/-}$ keratinocytes were apparent in vitro. MK6b expression under cell culture conditions was negligible, with less than 0.5% of MK6a$^{-/-}$ keratinocytes expressing MK6b in low-Ca^{2+} media, whereas MK6a was expressed in every cell of MK6a$^{+/+}$ cultures (not shown).

DISCUSSION

MK6a is necessary for fast reepithelialization from the hair follicle after wounding. To analyze a wound-healing process where the presence of the suprabasal MK6b isoform would not obscure a possible defect, we chose to look at reepithelialization from the hair follicle. The MK6a$^{-/-}$ mice indeed showed a clear delay in the kinetics of this process compared to wild-type mice. With the degree of reepithelialization as a gauge, 42-h-old tape-stripping wounds on MK6a$^{-/-}$ mice appear similar to 30-h-old wounds on MK6a$^{+/+}$ mice. MK6a$^{-/-}$ follicle reepithelialization could therefore be considered to lag behind MK6a$^{+/+}$ follicle reepithelialization a maximum of 12 h. While a delay of half a day or less may appear subtle, outside of the laboratory, especially with the potential for developing an infection, such a delay may translate into a difference in likelihood of survival.

Implications for the role of MK6 in keratinocyte proliferation. Having established that lack of MK6a impairs follicular reepithelialization, we wanted to assess whether this might be due to a defect in the proliferation rate or migration speed of the follicular keratinocytes. While K6, K16, and K17 are frequently described as hyperproliferation-associated keratins (16, 19), the MK6a-deficient mice make obvious the fact that this association does not mean that MK6 induction is necessary for proliferation of keratinocytes after wounding. In vivo BrdU labeling showed that the basal keratinocytes of the migrating epithelial tongue in full-thickness wounds proliferate in the absence of MK6 and so do the follicular keratinocytes of MK6a$^{-/-}$ mice, albeit with a delay in the onset of proliferation. Although the MK6a$^{-/-}$ follicles clearly had lower BrdU labeling indices than MK6a$^{+/+}$ follicles, this may indicate that migration and proliferation of follicular keratinocytes are closely linked, rather than indicating a primary proliferation defect. This interpretation is supported by the observation that, for both genotypes, the follicles that showed the most significant amount of reepithelialization tended to contain the highest number of BrdU-positive cells (not shown). In an organotypic wound-healing model, it has been demonstrated that the proliferative burst occurs after the onset of migration from the edge of a wound (8). It therefore appears possible that the delay in proliferation and migration of the follicular keratinocytes could be due to a primary defect in either the speed or onset of migration. If the ORS keratinocytes of the MK6a$^{-/-}$ mice were slower to migrate out of the follicle, this might cause a delay in proliferation if migration is necessary to stimulate proliferation.

Implications for keratinocyte migration in wound healing. While the delay in follicular reepithelialization could be explained by a migration defect, the absence of a migration defect in vitro and in the reepithelialization of full-thickness wounds argues against a prominent role of MK6a and also of MK6b in keratinocyte migration. The cultured keratinocytes were primarily derived from the epidermis, and migration out of the hair follicle cannot be accurately reproduced in vitro; however the MK6a$^{-/-}$ keratinocytes in full-thickness wounds were migrating in their native context of a three-dimensional wound bed. The in vivo staining pattern of the MK6a$^{-/-}$ epithelial tongue, with MK6b present only in suprabasal, BrdU-negative cells, is compatible with a model where the MK6b-positive cells were generated through displacement and differentiation from the pool of dividing cells below (23). We think it unlikely that the contribution of the MK6b-positive suprabasal cells to the progression of the epithelial tongue is an actual migration process. Once a keratin is expressed and assembled into the network, it is generally thought to be retained in the filament network even after expression ceases; for instance, the MK14 protein, which is expressed only in basal cells, is detected throughout the entire epidermis. Since the very tip and the bottom layers of the epithelial tongue were MK6b negative, migration of MK6b-positive cells would require that these cells migrate to the front and bottom of the tongue and then turn off MK6b expression and degrade the protein. A scenario where impairment of follicular reepithelialization is due to slower migration of MK6a$^{-/-}$ follicular keratinocytes therefore implies that migration of the cells out of the follicle has different requirements than migration in a full-thickness wound bed. Follicular and full-thickness reepithelialization might, for instance, differ in their requirements for MK16. Human K16 has been suggested to play a role in the onset of reepithelialization of full-thickness wounds through a rearrangement of the preexisting keratin network (30). Although this hypothesis was partly based on the in vitro properties of HK16 (30), which MK16 does not appear to share (32), both may still have similar in vivo roles. In the epithelial tongues of full-thickness wounds MK16 was induced in all suprabasal layers but only in isolated cells of the basal layer. As a consequence of this, two or three cell layers in the MK6a$^{-/-}$ epithelial tongue contain MK16 but not MK6. If K6 and K16 induction were critical for the migration of keratinocytes and if the network properties were indeed due to K16 alone (30), MK16, upon integration into the MK5/MK14 network, could impart its properties onto the keratin network even in the absence of MK6a. Since follicular reepithelialization was impaired in spite of the fact that MK16 was induced in part of the ORS (not shown), follicular and full-thickness reepithelialization may differ in their needs for not only MK6a but also MK16.

Implications for a potential role of MK6a in keratinocyte activation after wounding. Since migration and proliferation of MK6a$^{-/-}$ keratinocytes are not affected in vitro or in full-thickness wound healing, a possible explanation for the delay in follicular reepithelialization would be that the MK6a$^{-/-}$ follicular keratinocytes may be slower to be activated than wild-type cells but, once activated, migrate and divide at the same rates as wild-type cells. A primary effect of the MK6a protein on the structure and properties of the preexisting keratin network would qualify as a role for MK6a in keratinocyte activation. This scenario would, however, not explain why reepithelialization during anagen, when the ORS keratinocytes are already actively dividing and invading the connective tissue, was not delayed in the MK6a$^{-/-}$ mice. Although MK6a is not induced in the outer ORS during anagen, the follicular cells may already be in a state of activation similar to the one achieved after wounding, and all that is required is the redirection of migration towards the dermal surface. It therefore appears possible that there is some intersection between the presence of the MK6a protein in the ORS keratinocytes and the regulation of the migratory phenotype or potentially the cell cycle. We have no direct evidence for such a scenario, since it would require proof of a direct interaction between MK6a and a protein involved in signaling necessary for migration or cell cycle control, of which there are no reports for K6 or K16 and K17. However, another keratin, K18, has been shown to bind 14-3-3 proteins (18, 20), a protein family which has been shown to be involved in cell cycle control (6, 13). Furthermore, the colorectal hyperplasia observed in the K8 knockout mice in the FVB/N background points to a role for K8 in the proliferation or turnover rate of colon epithelial cells (2). It may therefore be of considerable interest to investigate whether K6, K16, and K17 can be shown to interact with proteins involved in cell cycle control or migration.

The delay in reepithelialization from the follicle in MK6a$^{-/-}$ mice is the first report of a keratin knockout mouse in which the phenotype is not related to degenerative changes or the hyperplastic response of the affected tissue. While we cannot entirely exclude the possibility that the absence of MK6a has a primary effect on the migration speed of the follicular keratinocytes, our data point to a role for MK6a induction in the activation of these cells after wounding.

ACKNOWLEDGMENTS

This work was supported by NIH grant HD25479.

We thank R. Porter and E. Lane for providing the MK16 antibody, A. Bradley for supplying the ES and SNL76/7 cells as well as the hprtΔ3′-neo vector, and P. Koch and J. Rothnagel for critical reading of the manuscript.

REFERENCES

1. **Albers, K., and E. Fuchs.** 1992. The molecular biology of intermediate filament proteins. Int. Rev. Cytol. **134:**243–279.
2. **Baribault, H., J. Penner, R. V. Iozzo, and M. Wilson-Heiner.** 1994. Colorectal hyperplasia and inflammation in keratin 8-deficient FVB/N mice. Genes Dev. **8:**2964–2973.
3. **Baribault, H., J. Price, K. Miyai, and R. G. Oshima.** 1993. Mid-gestational lethality in mice lacking keratin 8. Genes Dev. **7:**1191–1202.
4. **Bickenbach, J. R., M. A. Longley, D. S. Bundman, A. M. Dominey, P. E. Bowden, J. A. Rothnagel, and D. R. Roop.** 1996. A transgenic mouse model that recapitulates the clinical features of both neonatal and adult forms of the skin disease epidermolytic hyperkeratosis. Differentiation **61:**129–139.
5. **Blessing, M., H. Zentgraf, and J. L. Jorcano.** 1987. Differentially expressed bovine cytokeratin genes. Analysis of gene linkage and evolutionary conservation of 5′-upstream sequences. EMBO J. **6:**567–575.
6. **Chan, T. A., H. Hermeking, C. Lengauer, K. W. Kinzler, and B. Vogelstein.** 1999. 14-3-3 sigma is required to prevent mitotic catastrophe after DNA damage. Nature **401:**616–620.
7. **Corden, L. D., and W. H. McLean.** 1996. Human keratin diseases: hereditary fragility of specific epithelial tissues. Exp. Dermatol. **5:**297–307.
8. **Garlick, J. A., and L. B. Taichman.** 1994. Fate of human keratinocytes during reepithelialization in an organotypic culture model. Lab. Investig. **70:**916–924.
9. **Gillies, R. J., N. Didier, and M. Denton.** 1986. Determination of cell number in monolayer cultures. Anal. Biochem. **159:**109–113.
10. **Harper, J. R., D. A. Greenhalgh, and S. H. Yuspa.** 1988. Expression of transfected DNA by primary murine keratinocytes. J. Investig. Dermatol. **91:**150–153.
11. **Hatzfeld, M., and K. Weber.** 1990. The coiled coil of in vitro assembled keratin filaments is a heterodimer of type I and II keratins: use of site-specific mutagenesis and recombinant protein expression. J. Cell Biol. **110:** 1199–1210.
12. **Heins, S., and U. Aebi.** 1994. Making heads and tails of intermediate filament assembly, dynamics and networks. Curr. Opin. Cell Biol. **6:**25–33.
13. **Hermeking, H., C. Lengauer, K. Polyak, T. C. He, L. Zhang, S. Thiagalingam, K. W. Kinzler, and B. Vogelstein.** 1997. 14-3-3 sigma is a p53-regulated inhibitor of G2/M progression. Mol. Cell **1:**3–11.
14. **Ito, M.** 1986. The innermost cell layer of the outer root sheath in anagen hair follicle: light and electron microscopic study. Arch. Dermatol. Res. **279:**112–119.
15. **Ito, M.** 1988. Electron microscopic study on cell differentiation in anagen hair follicles in mice. J. Investig. Dermatol. **90:**65–72.
16. **Jiang, C. K., T. Magnaldo, M. Ohtsuki, I. M. Freedberg, F. Bernerd, and M. Blumenberg.** 1993. Epidermal growth factor and transforming growth factor alpha specifically induce the activation- and hyperproliferation-associated keratins 6 and 16. Proc. Natl. Acad. Sci. USA **90:**6786–6790.
17. **Kao, W. W., C. Y. Liu, R. L. Converse, A. Shiraishi, C. W. Kao, M. Ishizaki, T. Doetschman, and J. Duffy.** 1996. Keratin 12-deficient mice have fragile corneal epithelia. Investig. Ophthalmol. Vis. Sci. **37:**2572–2584.
18. **Ku, N. O., J. Liao, and M. B. Omary.** 1998. Phosphorylation of human keratin 18 serine 33 regulates binding to 14-3-3 proteins. EMBO J. **17:**1892–1906.
19. **Leigh, I. M., H. Navsaria, P. E. Purkis, I. A. McKay, P. E. Bowden, and P. N. Riddle.** 1995. Keratins (K16 and K17) as markers of keratinocyte hyperproliferation in psoriasis in vivo and in vitro. Br. J. Dermatol. **133:**501–511.
20. **Liao, J., and M. B. Omary.** 1996. 14-3-3 proteins associate with phosphorylated simple epithelial keratins during cell cycle progression and act as a solubility cofactor. J. Cell Biol. **133:**345–357.
21. **Lloyd, C., Q. C. Yu, J. Cheng, K. Turksen, L. Degenstein, E. Hutton, and E. Fuchs.** 1995. The basal keratin network of stratified squamous epithelia: defining K15 function in the absence of K14. J. Cell Biol. **129:**1329–1344.
22. **Magin, T. M., R. Schroder, S. Leitgeb, F. Wanninger, K. Zatloukal, C. Grund, and D. W. Melton.** 1998. Lessons from keratin 18 knockout mice: formation of novel keratin filaments, secondary loss of keratin 7 and accumulation of liver-specific keratin 8-positive aggregates. J. Cell Biol. **140:** 1441–1451.
23. **Matoltsy, A. G., and C. B. Viziam.** 1970. Further observations on epithelialization of small wounds: an autoradiographic study of incorporation and distribution of 3H-thymidine in the epithelium covering skin wounds. J. Investig. Dermatol. **55:**20–25.
24. **McGowan, K. M., and P. A. Coulombe.** 1998. Onset of keratin 17 expression coincides with the definition of major epithelial lineages during skin development. J. Cell Biol. **143:**469–486.
25. **McMahon, A. P., and A. Bradley.** 1990. The Wnt-1 (int-1) proto-oncogene is required for development of a large region of the mouse brain. Cell **62:**1073–1085.
26. **Moll, R., W. W. Franke, D. L. Schiller, B. Geiger, and R. Krepler.** 1982. The catalog of human cytokeratins: patterns of expression in normal epithelia, tumors and cultured cells. Cell **31:**11–24.
27. **Navarro, J. M., J. Casatorres, and J. L. Jorcano.** 1995. Elements controlling the expression and induction of the skin hyperproliferation-associated keratin K6. J. Biol. Chem. **270:**21362–21367.
28. **Ness, S. L., W. Edelmann, T. D. Jenkins, W. Liedtke, A. K. Rustgi, and R. Kucherlapati.** 1998. Mouse keratin 4 is necessary for internal epithelial integrity. J. Biol. Chem. **273:**23904–23911.
29. **Orwin, D. F.** 1971. Cell differentiation in the lower outer sheath of the Romney wool follicle: a companion cell layer. Aust. J. Biol. Sci. **24:**989–999.
30. **Paladini, R. D., K. Takahashi, N. S. Bravo, and P. A. Coulombe.** 1996. Onset of reepithelialization after skin injury correlates with a reorganization of keratin filaments in wound edge keratinocytes: defining a potential role for keratin 16. J. Cell Biol. **132:**381–397.
31. **Panteleyev, A. A., R. Paus, R. Wanner, W. Nurnberg, S. Eichmuller, R. Thiel, J. Zhang, B. M. Henz, and T. Rosenbach.** 1997. Keratin 17 gene expression during the murine hair cycle. J. Investig. Dermatol. **108:**324–329.
32. **Porter, R. M., A. M. Hutcheson, E. L. Rugg, R. A. Quinlan, and E. B. Lane.** 1998. cDNA cloning, expression, and assembly characteristics of mouse keratin 16. J. Biol. Chem. **273:**32265–32272.
33. **Porter, R. M., S. Leitgeb, D. W. Melton, O. Swensson, R. A. Eady, and T. M. Magin.** 1996. Gene targeting at the mouse cytokeratin 10 locus: severe skin fragility and changes of cytokeratin expression in the epidermis. J. Cell Biol. **132:**925–936.
34. **Ramirez-Solis, R., A. C. Davis, and A. Bradley.** 1993. Gene targeting in embryonic stem cells. Methods Enzymol. **225:**855–878.
35. **Ramirez-Solis, R., P. Liu, and A. Bradley.** 1995. Chromosome engineering in mice. Nature **378:**720–724.
36. **Ramirez-Solis, R., J. Rivera-Perez, J. D. Wallace, M. Wims, H. Zheng, and A. Bradley.** 1992. Genomic DNA microextraction: a method to screen numerous samples. Anal. Biochem. **201:**331–335.
37. **Roop, D. R., C. K. Cheng, L. Titterington, C. A. Meyers, J. R. Stanley, P. M. Steinert, and S. H. Yuspa.** 1984. Synthetic peptides corresponding to keratin subunits elicit highly specific antibodies. J. Biol. Chem. **259:**8037–8040.
38. **Rothnagel, J. A., T. Seki, M. Ogo, M. A. Longley, S. M. Wojcik, D. S. Bundman, J. R. Bickenbach, and D. R. Roop.** 1999. The mouse keratin 6 isoforms are differentially expressed in the hair follicle, footpad, tongue and activated epidermis. Differentiation **65:**119–130.
39. **Smith, F. J., V. A. McKusick, K. Nielsen, E. Pfendner, J. Uitto, and W. H. McLean.** 1999. Cloning of multiple keratin 16 genes facilitates prenatal diagnosis of pachyonychia congenita type 1. Prenatal Diagn. **19:**941–946.
40. **Steinert, P. M.** 1990. The two-chain coiled-coil molecule of native epidermal keratin intermediate filaments is a type I-type II heterodimer. J. Biol. Chem. **265:**8766–8774.
41. **Steinert, P. M., and D. R. Roop.** 1988. Molecular and cellular biology of intermediate filaments. Annu. Rev. Biochem. **57:**593–625.
42. **Takahashi, K., and P. A. Coulombe.** 1996. A transgenic mouse model with an inducible skin blistering disease phenotype. Proc. Natl. Acad. Sci. USA **93:**14776–14781.
43. **Takahashi, K., R. D. Paladini, and P. A. Coulombe.** 1995. Cloning and characterization of multiple human genes and cDNAs encoding highly related type II keratin 6 isoforms. J. Biol. Chem. **270:**18581–18592.
44. **Takahashi, K., B. Yan, K. Yamanishi, S. Imamura, and P. A. Coulombe.** 1998. The two functional keratin 6 genes of mouse are differentially regulated and evolved independently from their human orthologs. Genomics **53:**170–183.
45. **Troyanovsky, S. M., R. E. Leube, and W. W. Franke.** 1992. Characterization of the human gene encoding cytokeratin 17 and its expression pattern. Eur. J. Cell Biol. **59:**127–137.
46. **Winter, H., L. Langbein, S. Praetzel, M. Jacobs, M. A. Rogers, I. M. Leigh, N. Tidman, and J. Schweizer.** 1998. A novel human type II cytokeratin, K6hf, specifically expressed in the companion layer of the hair follicle. J. Investig. Dermatol. **111:**955–962.
47. **Wojcik, S. M., S. Imakado, T. Seki, M. A. Longley, L. Petherbridge, D. S. Bundman, J. R. Bickenbach, J. A. Rothnagel, and D. R. Roop.** 1999. Expression of MK6a dominant-negative and C-terminal mutant transgenes in mice has distinct phenotypic consequences in the epidermis and hair follicle. Differentiation **65:**97–112.